# Effect of Winding Asymmetries and Winding Connection on Small Synchronous Machines

David G. Dorrell[1]
Senior Member

[1]University of Technology Sydney
Faculty of Engineering and IT
Broadway, Sydney, NSW 2007 Australia
e-mail david.dorrell@uts.edu.au

Mircea Popescu[2]
Senior Member

[2]Motor Design Ltd
Ellesmere, Shropshire, SY12 0EG, UK
e-mail mircea.popescu@motor-design.com

***Abstract* -- This paper reports on the study of winding asymmetries in small synchronous generators. These types of generator are commonly used in diesel generator or back-up systems and are usually no more than a few or few tens of kilowatts with two, four or six salient poles. The 3-phase winding is 120 deg pitched but often lap windings are not used, rather a hybrid of concentric winding and double layering is utilized. There are sound manufacturing reasons for this and these are explained. This leads to small asymmetries in the phase-belt inductances and field-induced voltages. This is examined and validated experimentally. The paper discusses the techniques that are used to analyze the machine. These are analytical methods. The methods address the correct positional coil groupings in the slots to obtain back-EMFs, mutual and self-inductances and line currents. These are obtained over a varying load range.**

***Index Terms*—Inductance, synchronous machines, windings.**

## I. INTRODUCTION

Small synchronous machines are the extensively used in small diesel- or petrol-driven generator sets. The size of these sets is variable from a few hundred watts up to a few megawatts. These machines can be two pole machines (smaller machines and even single phase systems) but are generally four or six poles in the larger units. These will correspond to operating speeds of the diesel or petrol engine. In induction motors, smaller machines tend to have single layer concentric windings (which is essentially a fully-pitched winding) while larger machines have far more slots and will be double-layer lap windings with possibly one or two slot short pitching. Double-layer lap windings in 3-phase rotating machines are usually used to introduce this short pitching for MMF winding harmonic elimination. In a synchronous generator is it important to investigate the winding harmonics to reduce generated EMF harmonics. Skew can reduce higher harmonics; however, in generators, elimination of the 3$^{rd}$ harmonic is important. In smaller synchronous machines 2/3$^{rd}$ pitching is necessary to remove the 3$^{rd}$ harmonics, and illustrations of this are given in [1] and [2]. Symmetry is also necessary as illustrated in [3]. In this paper, an alternative to the lap winding is described and the asymmetry investigated. This arrangement has been used extensively in production machines successfully for many years. The asymmetry is small and occasionally can generate an anomalous issue during operation. Asymmetries were investigated in larger low-speed generators in [4] and many different variations possible in the layout.

## II. WINDING ARRANGEMENTS

In this section the different possible winding arrangements are investigated and issues with their assembly and asymmetry are highlighted. These windings are aimed at

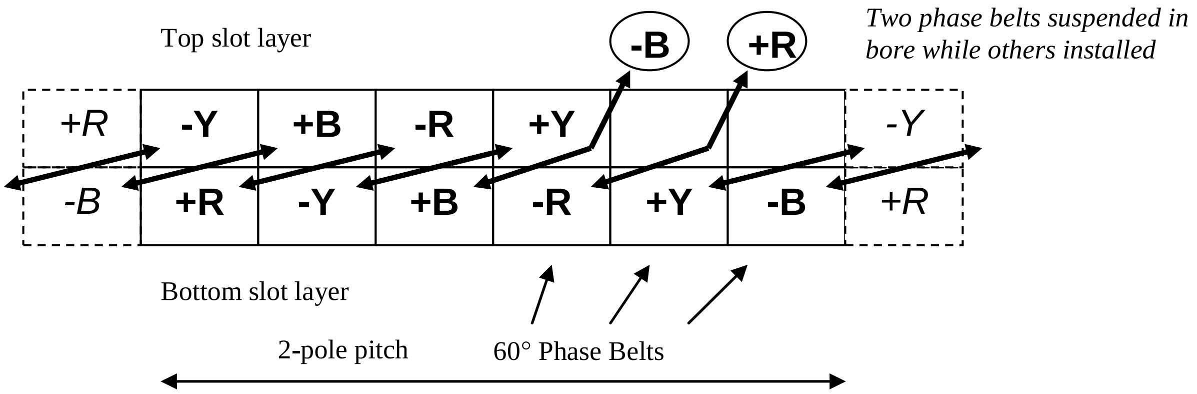


Fig. 1. Winding diagram illustrating double-layer 2/3$^{rd}$ pitched lap winding and the necessity for coil-side suspension while complete winding is inserted.

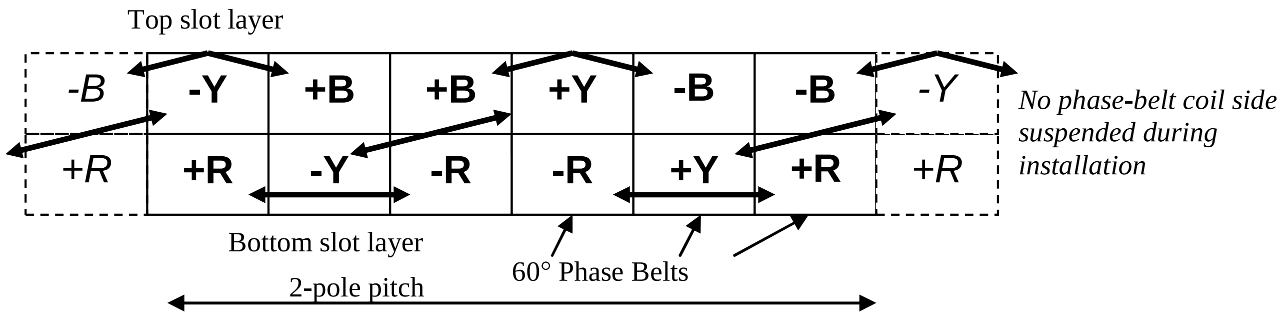


Fig. 2. Winding diagram illustrating hybrid concentric double-layer 2/3rd pitched winding – all coils can be inserted completely in the insertion sequence Red – Yellow - Blue.

realizing 2/3$^{rd}$ pitching to eliminate the 3$^{rd}$ harmonic voltages. First the more usual lap winding is assessed in terms of assembly then the hybrid double-layer concentric winding is assessed to overcome the assembly issues.

### *A. Short Pitched Lap Windings*

Lap windings require hand winding and coils sides have to be left hanging when starting the winding. Only when the finishing coils are inserted can the hanging coil sides be fitted into the top section of the slot. This is illustrated in Fig. 1. The main problem with this is that having two phase-belt-side groups hanging in the bore can be very cumbersome during manufacture in modern compact machines with high torque densities. In smaller generators (a few tens of kilowatts) then it can be difficult to fit this winding and there is potential for damaging the winding during fitting. An alternative is the hybrid double-layer concentric winding as described in the next section and this winding will be the focus of this paper.

### *B. Hybrid Double-Layer Concentric Winding*

In smaller synchronous machines semi-automated winding is required to reduce manufacturing costs. As already discussed, these machines are usually of a few or few tens of kilowatts and of two, four or six salient poles so that have can be matched to small two-stroke engines (in very small generators) or diesel engines for 50 Hz or 60 Hz generation in back-up or auxiliary generation sets. These sets can be stand-alone or grid-connected. The rotors in these machines tend to be salient pole rotors, with long or short damper cages.

Automated winding techniques can be applied to concentric windings which are usually single layer. The problem with single layer windings is that they cannot be short pitched to eliminate time harmonics in the terminal EMF.

However, in a 2/3$^{rd}$ pitched synchronous machine it is possible to use a hybrid concentric double-layer winding layout to ease construction. Fig. 2 shows this arrangement. When winding a machine with this arrangement, the phase coils for the first (Red) phase are put wholly in the bottom of the slots. The second phase coils (Yellow) are put in top-to-bottom slot locations and the third (Blue) phase coils are fitted in the top of the slots. This can be followed in Fig. 2 (which is a minor correction from [5]). The advantage to this arrangement is that phase-belt coil-side groupings are never left suspended in the bore while other phase-belt coil-sides are installed. The end-winding, while not having the symmetrical and neat arrangement that is present in the lap winding, is still straightforward to assemble and it is compact. The disadvantage is that there will be asymmetries between the phases that will lead to slight variations in the field-EMF magnitudes induced into the phase belts and different phase-belt leakage inductances (both self and mutual slot leakages). The main asymmetry will be the coil-side slot inductances (self and mutual) but there will also be small asymmetries in the end-winding self and mutual inductances.

### *C. Twin Single-Layer Windings*

An alternative to the hybrid double-layer winding is the twin single-layer winding as discussed here.

This paper highlights the effects of small winding asymmetries in small synchronous machine; there is a third winding arrangement that can also produce asymmetries. This arrangement uses two single-layer concentric windings and pitches them by sixty degrees with respect to each other to effect a 2/3$^{rd}$ pitching. This was studied in [6] and is illustrated in Fig. 3 (which is a minor correction from [5]). This is effectively formed from two single-layer concentric windings that are offset by 60 electrical degrees. This should be a good winding if the layers are series-connected but if an attempt is made to parallel-connect the layers then large circulating currents will occur as illustrated in [6]. In addition, the end-winding arrangement will not be compact.

## III. Analysis

The main emphasis of this paper will be the winding in Fig. 2 and the different analysis methods will be reviewed in the sections below. Analytical analysis is used to help understand the problem. Finite element analysis can be used to obtain finer detailing. The simulation work will be validated with experimental results as illustrated below.

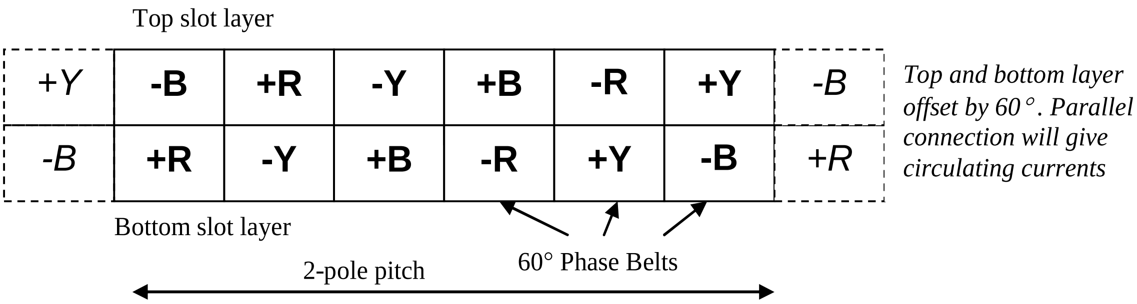


Fig. 3. 2/3rd pitched winding formed from twin single-layer windings connected in series.

### *A. Analysis Possibilities and Approach*

The analysis is couched in terms of analytical calculations which are implemented in MATLAB. However, it is possible to validate and calculate more accurate values when either static or time-stepped finite element analysis is implemented using techniques such as the "frozen permeabilities" method [7] to break the flux down into different components to obtain the field-EMFs and inductances. To model the machine either 2D finite element analysis can be used with lumped circuit analysis for the end-winding inductances, or a full 3D analysis carried out, which can be very demanding on computing power. For 2D analysis, iterative analytical methods such as [8] can be used to obtain good end-winding calculations.

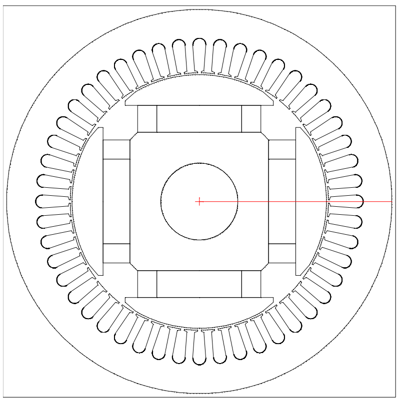

Fig. 4. General salient 4-pole 48-slot geometry.

In the first instance, the machine winding arrangement will be considered then the analysis will be put forward. Fig. 4 gives a general cross-section arrangement for a small four-pole synchronous machine. Fig. 5 shows one phase of a double layer winding for the 4-pole machine in Fig. 4 – this has 2/3rd pitching. However, the experimental work uses a Mawdsley's Generalized Machine [9] (set up in a 2-pole arrangement) which is used for method validation as described below – the winding is far from ideal but it illustrates the asymmetry in top/bottom layering of the hybrid double-layer concentric winding. Several companies have produced generalized machines. Several of these were reviewed by Ellison (machines by A.E.I. Ltd., B.K.B. Electric Motors Ltd., Mawdsley's Ltd. and Westinghouse Electric Corp.) [10].

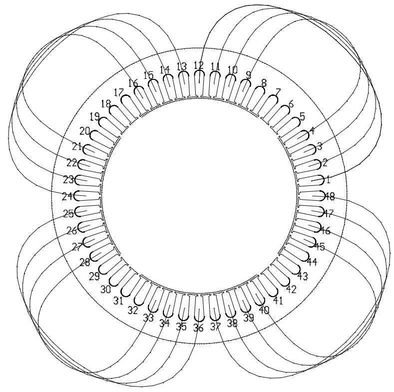

Fig. 5. Phase winding layout for one phase.

These generalized machines were popular in the 1950s and 1960s and were used in extended university courses on electrical machines which taught generalized machines concepts. They have now lost popularity. The Mawdsley's machine used here is described below; it has 48 slots with 48 lap coils in two 24-coil single layer coils sets. Each coil comes out to an individual pair of terminals to allow multiple stator winding connections. These allow three-phase windings for ac machine representations or coil connections for DC motor field connection. The rotor is a more complex structure with 36 slots. At one end is a commutator with four retractable brushes and the coils are pitched by 12 slots (full pitching for a 4 pole machine). This allows a 4 pole DC motor armature operation. Each brush is connected via a slip ring and the brushes can either be locked stationary or locked to the rotor. When locked to the rotor this allows a 4-pole round-rotor synchronous machine to be simulated (as used here). At the other end is a set of 6 tapings accessible by brushes which allow a 6-pole synchronous machine rotor or 4 pole wound rotor induction motor. There is a shorting ring for the commutator; a cage type-structure is represented by shorting the commutator and removing the 6 brushes at the other end. These arrangements represent the concept of the different motor forms but do not form a high performance representation due to the design compromises necessary in a generalized machine, hence their drop in popularity. However, they are quire adequate for testing concepts as illustrated in this paper and also in [11].

### *B. Winding Connection*

It is now worth briefly reviewing the possible connections. The review is in terms of a 50 Hz low voltage machine but the numbers are similar for a 60 Hz machine. A small synchronous machine is often designed to allow multiple voltage operation by reconnection of the phase belts. If sixty-degree phase belts are used then there will be one phase belt per pole. There are numerous ways to connect the machine. These are generally star, delta, multiple-star, multiple-delta or zig-zag (for single phase operation). Taking the simple case of a two-pole machine where there are two coil groupings per phase, several connections are possible (assuming the series star to be the most popular 415 V line rating) as given in Table I.

TABLE I
WINDING CONNECTIONS FOR SMALL SYNCHRONOUS MACHINES

| Phase Number | Connection | Line Voltage |
|---|---|---|
| 3-phase | Series star | 415 V |
| | Parallel star | 207 V |
| | Series delta | 240 V |
| | Parallel delta | 120 V |
| Single-phase | Series zig-zag | 480 V |
| | Parallel zig-zag | 240 V |

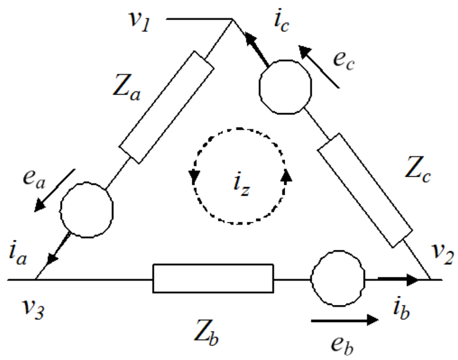

Fig. 6. Delta generator connections with current definitions.

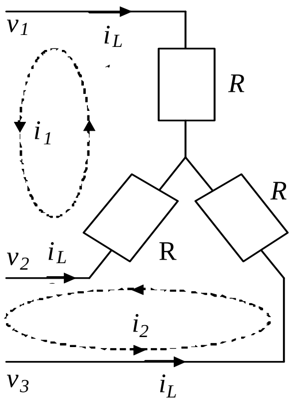

Fig. 7. Star load connection showing loop currents used in analysis (this is connected to the generator in Fig. 6).

The asymmetrical hybrid double-layer concentric winding can be connected in either a delta or star configuration but delta is used in the experimental work. The delta connection allows circulating currents around the mesh as illustrated in Fig. 6.

### *C. Open Circuit Analysis – Delta Connection*

If the generator is balanced there will be no zero-order circulating current $i_z$ in the delta in Fig. 6. Note that we are using the motoring convention here with the generator line current $i_{L1(G)}$ flowing into the machine and equal $i_a - i_c$. However, if there is an imbalance in the excitation voltages $e_a$, $e_b$, and $e_c$ then there will be a circulating current $i_z$ and it is necessary to calculate this. The open-circuit zero-order current can be calculated as follows assuming the circuit is as shown in Fig. 6 (where the impedance $Z$ represents both self and mutual terms). The excitation voltages (induced by the rotating rotor flux) will vary in magnitude but should be 120° out of phase with respect to each other. This is because the imbalance is due to the positioning of the coil in the slots which will affect the linkage. If the coil sides of a coil are in the top of the slots (in a double layer winding) then there will be a slightly higher linkage with the rotor flux compared to a coil with coil-sides in the bottom of the slots. Hence, there will be a variation in linkage, i.e., voltage magnitude, rather than a shift in phase. Therefore:

$$\begin{aligned} e_a(t) &= \mathrm{Re}\left\{E_a e^{j\omega t}\right\} = \mathrm{Re}\left\{(E-\Delta E_a)e^{j\omega t}\right\} \\ &= \mathrm{Re}\left\{(E-\Delta V)e^{j\omega t}\right\}; \\ e_b(t) &= \mathrm{Re}\left\{E_b e^{j\omega t}\right\} = \mathrm{Re}\left\{a^2 E-\Delta E_b e^{j\omega t}\right\} \\ &= \mathrm{Re}\left\{a^2 E e^{j\omega t}\right\} \text{ and} \\ e_c(t) &= \mathrm{Re}\left\{E_c e^{j\omega t}\right\} = \mathrm{Re}\left\{a(E-\Delta E_c)e^{j\omega t}\right\} \\ &= \mathrm{Re}\left\{a(E+\Delta V)e^{j\omega t}\right\} \end{aligned} \tag{1}$$

where the operator $a = e^{j2/3}$ and a balanced three-phase excitation phasor set is $E$, $a^2E$ and $aE$, where each coil is assumed to have one coil-side in the top of a slot and one coil-side in the bottom of the slot. If phase $a$ has all its coil-sides in the bottom of the slots then there will be a reduction in voltage $\Delta E_a$ which will be equal to $\Delta V$. Phase $b$ will not have a change in voltage because half the coil-sides are in the top of the slots and half in the bottom, so that $\Delta E_b = 0$. For phase $c$ all the coil-sides are in the top of the slots so that the voltage will increase, hence $\Delta E_c = -\Delta V$.

The phase impedances have main (subscript $S$ for self inductances and $M$ for mutual inductances) and leakage (subscript $L$) reactances. The phases are assumed to have the same resistance. The line-to-line voltages are then

$$\begin{aligned}\overline{V}_1-\overline{V}_2 &= \overline{V}_a = \overline{Z}_a\overline{I}_a + \overline{Z}_{Mab}\overline{I}_b + \overline{Z}_{Mac}\overline{I}_c \\ &= \left\{R_{ph} + j(X_S + X_{La})\right\}\overline{I}_a - jX_M\left(\overline{I}_b + \overline{I}_c\right); \\ \overline{V}_2-\overline{V}_3 &= \overline{V}_b = \overline{Z}_b\overline{I}_b + \overline{Z}_{Mba}\overline{I}_a + \overline{Z}_{Mbc}\overline{I}_c \\ &= \left\{R_{ph} + j(X_S + X_{Lb})\right\}\overline{I}_b - jX_M\left(\overline{I}_a + \overline{I}_c\right); \\ \overline{V}_3-\overline{V}_1 &= \overline{V}_c = \overline{Z}_c\overline{I}_c + \overline{Z}_{Mca}\overline{I}_a + \overline{Z}_{Mcb}\overline{I}_b \\ &= \left\{R_{ph} + j(X_S + X_{Lc})\right\}\overline{I}_c - jX_M\left(\overline{I}_a + \overline{I}_b\right)\end{aligned} \tag{2}$$

This assumes that the slot mutuals and the end-winding mutuals are neglected. For the zero-order driving voltage on open circuit (mains frequency, not 3rd harmonic):

$$\begin{aligned} v_{z(oc)}(t) &= e_a + e_b + e_c = \mathrm{Re}\left\{(a-1)\Delta V e^{j\omega t}\right\} \\ \left|v_{z(oc)}\right| &= \sqrt{3}\Delta V \end{aligned} \tag{3}$$

The impedance for the zero-order current round the delta mesh when open circuit is

$$\overline{Z} = 3\left\{R_{ph} + j\left(X_s - 2X_M\right)\right\} + j\left(X_{La} + X_{Lb} + X_{Lc}\right) \tag{4}$$

since $\overline{I}_a = \overline{I}_b = \overline{I}_c$ for open-circuit conditions. If the mutual reactance magnitude is half the self inductance then the main self and mutual reactances cancel, and we can write the open-circuit circulating current as

$$\overline{I}_z(oc) = \frac{\sqrt{3}\Delta V}{3R_{ph} + j\left(X_{La} + X_{Lb} + X_{Lc}\right)} \tag{5}$$

Hence, the open-circuit circulating current is therefore a function on the imbalance in voltage, winding resistance and the leakage reactance. If there is no imbalance in excitation voltage, so that $\Delta V$ = 0, there is no circulating current. However, if the generator is loaded there will be an imbalance in line currents and circulating current $i_z$. The next section calculates this.

For the Mawdsley's Test Machine used in the experimental validation, the current is predicted to be 0.29 A, and measured at 0.22 A (this was obtained by opening the delta with no load and measuring the individual phase voltages). This is fair correlation. In larger machines, where the p.u. resistance and reactance can be low, then the circulating current could be much higher.

### *D. Load Analysis – Star Connection*

To analyze the mesh with a star load on it is necessary to implement a mesh analysis. The additional load circuit components are shown in Fig. 7.

The load is a three-phase variable-resistor load bank and the three loop currents $i_1$, $i_2$ and $i_Z$ fully describe all the current paths, from which the line and phase currents can be derived. For the generator connection in Fig. 6 and motor connection in Fig. 7, an impedance matrix can be obtained from

$$\begin{bmatrix} e_a \\ e_b \\ e_c \end{bmatrix} = \begin{bmatrix} \overline{Z}_{11}\overline{Z}_{12}\overline{Z}_{13} \\ \overline{Z}_{21}\overline{Z}_{22}\overline{Z}_{23} \\ \overline{Z}_{31}\overline{Z}_{32}\overline{Z}_{33} \end{bmatrix} \begin{bmatrix} i_1 \\ i_2 \\ i_z \end{bmatrix} \tag{6}$$

where the current loops are shown in Figs. 6 and 7. As an example

$$\begin{aligned} e_a &= \left\{R_{ph} + j(X_S + X_{La})\right\} i_a - jX_M(i_b + i_c) + Ri_1 + Ri_2 \\ &= \left\{R_{ph} + j(X_S + X_{La})\right\} i_z - jX_M(-i_2 - i_1) + Ri_1 + Ri_2 \\ &= \left(R + jX_M\right)(i_1 + i_2) + \left\{R_{ph} + j(X_S + X_{La})\right\} i_z \\ &= \overline{Z}_{11}i_1 + \overline{Z}_{12}i_2 + \overline{Z}_{13}i_z \end{aligned} \tag{7}$$

Similar equations exist for $e_b$ and $e_c$. Equation (6) is inverted to obtain the currents. The phase currents can be obtained from a connection matrix, further use of a connection matrix then yields the forward and backward current components. This is illustrated in (8) and (9) below. Addressing Figs. 6 and 7, the phase currents in the generator $i_a$, $i_b$ and $i_c$ can be related to the circulating currents in the load $i_1$ and $i_2$ and the zero order current in generator delta $i_z$ using

$$\begin{bmatrix} i_a \\ i_b \\ i_c \end{bmatrix} = \begin{bmatrix} 0 & 0 & 1 \\ 0 & -1 & 1 \\ -1 & 1 & 1 \end{bmatrix} \begin{bmatrix} i_1 \\ i_2 \\ i_z \end{bmatrix} \tag{8}$$

The generator phase currents can be transformed into forwards, backwards and zero order currents $i_{f(ph)}$, $i_{b(ph)}$ and $i_{z(ph)}$ where

$$\begin{bmatrix} i_{f(ph)} \\ i_{b(ph)} \\ i_{z(ph)} \end{bmatrix} = \frac{1}{3} \begin{bmatrix} 1 & a & a^2 \\ 1 & a^2 & a \\ 1 & 1 & 1 \end{bmatrix} \begin{bmatrix} i_a \\ i_b \\ i_c \end{bmatrix} \tag{9}$$

The load line currents $i_{L1}$, $i_{L2}$ and $I_{L3}$ can be obtained from

$$\begin{bmatrix} i_{L1} \\ i_{L2} \\ i_{L3} \end{bmatrix} = \begin{bmatrix} -1 & 0 & 0 \\ 1 & -1 & 0 \\ 0 & 1 & 0 \end{bmatrix} \begin{bmatrix} i_1 \\ i_2 \\ i_Z \end{bmatrix} \tag{10}$$

And these can also be transformed into the load forwards, backwards and zero order currents $i_{fL(ph)}$, $i_{bL(ph)}$ and $i_{zL(ph)}$ so that

$$\begin{bmatrix} i_{fL} \\ i_{bL} \\ i_{zL} \end{bmatrix} = \frac{1}{3} \begin{bmatrix} 1 & a & a^2 \\ 1 & a^2 & a \\ 1 & 1 & 1 \end{bmatrix} \begin{bmatrix} i_{L1} \\ i_{L2} \\ i_{L3} \end{bmatrix} \tag{11}$$

The zero-order line current should be zero since the star point is not earthed. It should also be noted that International Standard IEC 60034-1 specifies that the machine should be able to operate continuously on an unbalanced load, where

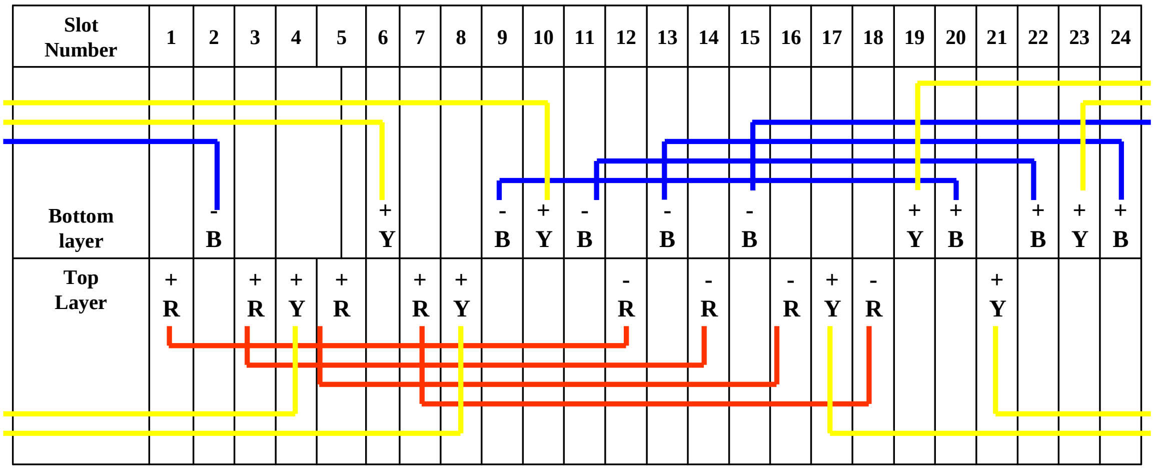


Fig. 8. Winding layout for half of stator slots in the Mawdsley machine.

the amount of allowable reverse sequence current is between 5 and 10 % depending on the type of machine, so obtaining these is very necessary.

The algorithm was implemented in MATLAB and some results are given in the next section. The components will be calculated analytically then validated experimentally.

## IV. Experimental Validation

The algorithm was tested using a Mawdsley's Generalised Machine (MGM) Set arranged as a synchronous machine [8] in a two-pole form arrangement.

### *A. Machine parameters*

The relevant parameters necessary for the analysis are given in Table II. The main difference between this experimental set-up and an actual hybrid double-layer concentric machine is that there is no mutual slot leakage between the different phases due to the nature of the winding layout. However, this is very small compared to the main mutual inductance.

TABLE II
Mawdsley Machine Parameters

| Parameter | Red phase | Yellow Phase | Blue Phase |
|---|---|---|---|
| Open circuit phase voltage [V] | 161.1 | 163 | 165.1 |
| Slot leakage inductance [mH] | 6.27 | 4.51 | 2.74 |
| End leakage inductance [mH] | 3.2 | 3.2 | 3.2 |
| Main self inductance [mH] | 420 | 420 | 420 |
| Mutual inductance [mH] | 210 | 210 | 210 |
| Phase resistance [Ohms] | 3.2 | 3.2 | 3.2 |

The MGM consisted of two single-layer windings in 48 slots. Therefore there were 24 coils per layer and the coil pitch was 11 slots. To simulate the effect of having phase bands wholly on the bottom, top-to-bottom and top only then the machine coils were connected as shown in Fig. 8 (half machine – the second half had same coil arrangement but reversed polarity). The rotor had a cylindrical rotor with 36 slots and this was connected to give a 2-pole air-gap flux wave with little 3$^{rd}$ harmonic content.

### *B. Delta Connection and Zero Order Current*

Since the stator winding is not a true 2/3$^{rd}$ pitch then this was necessary to minimize 3$^{rd}$ harmonic. The circulating zero-order current was checked for correct frequency to ensure it was not due to the 3$^{rd}$ harmonic. The machine speed and terminal voltage were kept constant and the load varied. The zero-order circulating current is shown in Fig. 9. The predictions are shown as an upper boundary and a lower boundary. These boundaries are set by $\Delta V$ in (1). The lower boundary keeps $\Delta V$ constant whatever excitation variation (via the field) and is set by the open circuit voltage measurements. The upper boundary is set by the scaling of $\Delta V$ with excitation (i.e. increasing with load). Good correlation was found since the measured currents lie within the two boundaries and it can be seen that the current circulating round the delta mesh increases slightly with load (reducing load resistance).

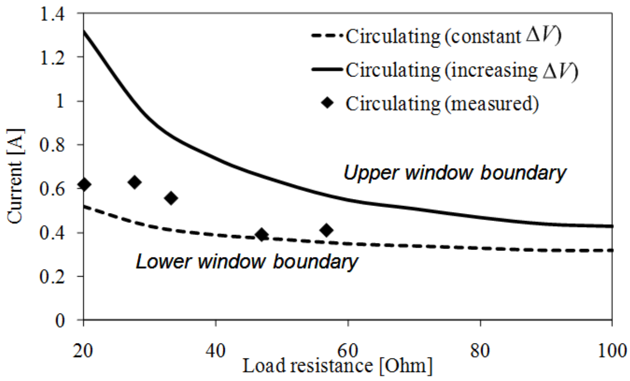


Fig. 9. Delta connection in Mawdsley machine – zero-order circulating current around delta winding.

*C. Delta Connection with Loading*

Fig. 10 shows the variation of the phase currents in the generator (keeping $\Delta V$ constant). Again, the measurements give good agreement and follow the general trends. The phase currents, when broken down into forward, backward and zero-order components revealed there to be little backward component. The line current, on the other hand, cannot contain zero-order due to the floating star point. Therefore these contained forward and backward components only. These are shown in Fig. 11. This also shows the backwards sequence component as a percentage of the forwards sequence component. As already stated, the International Standard IEC 60034-1 gives the maximum value of backwards sequence current that is allowed. In this machine it rises to over 25 % but is should be remembered that this is an experimental rig designed to highlight the effects of the asymmetry and these high backwards components occur at a very light load.

The spread of the currents when measured is not as marked as predicted however, there will be additional steel saturation and other effects that are not incorporated into the simple model. Additional effects included end-winding mutual variation and general connection asymmetries. Further work would be to model this machine using finite element analysis then extend the work to a production machine and testing of the loading effects in more detail. This is a substantial amount of work, particularly if end windings are included via the use of 3D finite element analysis. However, here we are simply putting forward a simple calculation method in order to allow rapid assessment of the currents and this is the sort of calculation that is easily implemented in the design office. The method is validated experimentally.

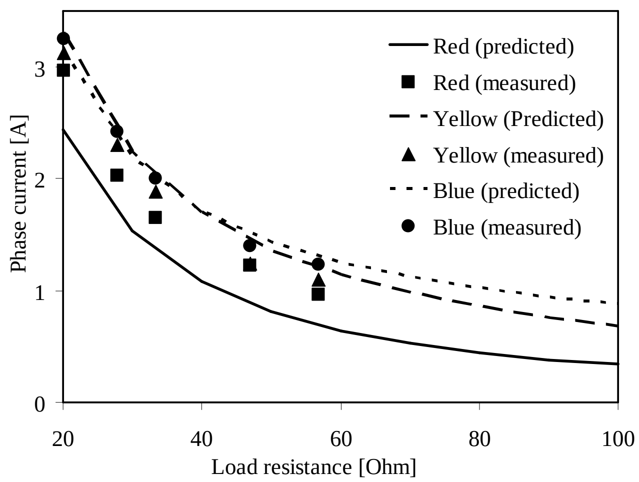


Fig. 10. Delta connection in Mawdsley machine – phase currents in generator.

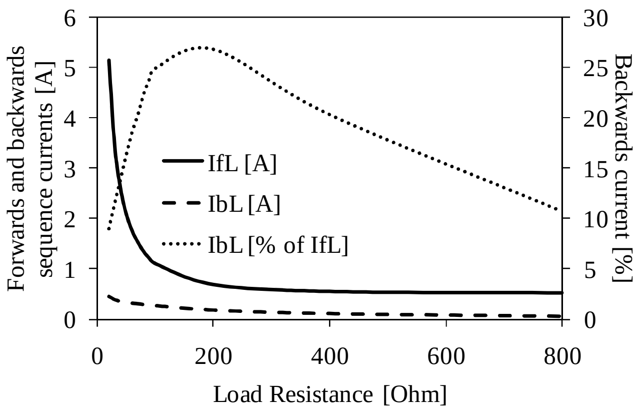


Fig. 11. Delta connection in Mawdsley machine – sequence line currents in load (zero-order is zero); the backwards is also shown as percentage of forwards sequence.

## V. Conclusions

This paper has put forward a simple model for a production winding technique in small synchronous machines that is slightly asymmetrical. The model was programmed in MATLAB and validated using experiments. The simulation results are put forward for an example laboratory machine; however, further work would be to expand and detail in more depth using a production machine. There is little recent literature about the operation of these small generators and the analysis of them using modern techniques. These machines are often expected to operate in a flexible mode when used in portable generator sets.

## Acknowledgment


Much of this work was carried out some time ago and the primary author is grateful to The University of Reading, UK, for their facilities and also to Prof. Lawrence Haydock, who was Technical Director of Newage International at that time, for his highlighting of the issue of asymmetrical windings.


## References


[1] I. Tabatabaei, J. Faiz, H. Lesani and M. T. Nabavi-Razavi, “Modeling and Simulation of a Salient-Pole Synchronous Generator With Dynamic Eccentricity Using Modified Winding Function Theory”, *IEEE Trans. on Magnetics*, Vol. 40, No. 3, May 2004, pp 1550 – 1555.

[2] H. A. Toliyat and N. A. Al-Nuaim, “Simulation and Detection of Dynamic Air-Gap Eccentricity in Salient-Pole Synchronous Machines”, *IEEE Trans. on Ind. Appl.*, Vol. 35, No. 1, Jan/Feb 1999, pp 86 – 93.

[3] X.Tu, L.-A. Dessaint, N. Fallati and B. De Kelper, “Modeling and Real-Time Simulation of Internal Faults in Synchronous Generators With Parallel-Connected Windings,” *IEEE Trans. on Ind. Electr.*, Vol 54, No. 3, June 2007, pp 1400 – 1409.

[4] Y. P. Liang, Y. P. Lu, W. Cai and B. J. Ge, “The Influence of Unequal Phase Belts in Stator Windings on Reactance of Large Waterwheel Generator”, *IEEE International Conference on Electric Machines and Drives Conference*, Vol.1, 1-4 June 2003, pp 411 – 414.

[5] D. G. Dorrell and M. Popescu, “Effect of Winding Asymmetries and Winding Connection on Small Synchronous Machines,” IEEE ECCE Conference, Sept 2010, pp 17 – 22.

[6] D. G. Dorrell, “Circulating Currents within Small Synchronous Generators”, *International Conference on Electrical Machines*, Istanbul, Turkey, Sept 2-4 1998, Vol 1, pp 14-19.

[7] J. A. Walker, D. Dorrell and C. Cossar, “Verification of the frozen permeabilites method for calculating the permanent-magnet motor”, *IEEE Trans. on Magnetics*, Vol. 41, No. 10, Oct. 2005, pp 3946 – 3948.

[8] D. Ban, D. Zarko, and I. Mandic, “Turbogenerator End-Winding Leakage Inductance Calculation Using a 3-D Analytical Approach Based on the Solution of Neumann Integrals, “ *IEEE Trans on Energy Appl.*, Vol. 20, No. 1, March 2005, pp 98 – 105.

[9] Mawdsley's Ltd., *The Multiform Experimental Sets*, UK 1967.

[10] A. J. Ellison, *Generalized Electric Machines*, George G. Harrap & Co. Ltd., London, UK, 1967.

[11] B. Singh, M. Singh, and A. K. Tandon, “Transient Performance of Series-Compensated Three-Phase Self-Excited Induction Generator Feeding Dynamic Loads,” *IEEE Trans on Ind. Appl*., vol. 46, no. 4 July/Aug 2010, pp 1271-1280.